where ω_1, ω_2, and ω_3 are the jump frequencies of: (1) host-atom jumps between two sites which are first neighbors to the impurity, (2) impurity-atom jumps, and (3) host-atom jumps away from the impurity. $F \approx 0.736$.

The formation energy for a vacancy next to a Kr atom is listed in Table II. We found this using E_v^0 for pure Ar, recognizing that now one Ar-Ar bond has been replaced by a Kr-Ar bond, and assuming that the relaxation remains unchanged. Then E_m^0, the migration energy in $\omega_a = C_a e^{-E_m^a/RT}$, is found using $E_m^0 = Q^0 - E_v^0$. To calculate f for Kr via the vacancy mechanism, we have used $E_m^2 = E_m^0$ (Kr in Ar), $E_m^1 = E_m^3 = E_m^0$ (self-diffusion), and taken $C_1 = C_2 = C_3$ although we expect $C_2 \lesssim C_1$. The resulting value of f for the (12,6) potential is listed in Table II.

Quite generally, since a Kr atom is larger than an Ar atom we expect $Q_{Kr} > Q_{Ar}$ so that, independent of potential arguments, we expect $f_{Kr} > f_{self}$ for a single-vacancy mechanism. This argument fails if there is a Kr-vacancy bond strong enough to cause the two to migrate as a bound pair.

PHYSICAL REVIEW VOLUME 188, NUMBER 3 15 DECEMBER 1969

Optical Absorption of Solid Krypton and Xenon in the Far Ultraviolet*

R. HAENSEL, G. KEITEL, AND P. SCHREIBER
Physikalisches Staatsinstitut, II. Institut für Experimentalphysik der Universität Hamburg, Hamburg, Germany

AND

C. KUNZ†
Deutsches Elektronen-Synchrotron, Hamburg, Germany

(Received 18 July 1969)

Photoabsorption caused by transitions of the $3d$ electrons in solid Kr and of the $4d$ and $4p$ electrons in solid Xe has been measured. The 7.5-GeV electron synchrotron DESY served as a light source. As a comparison, the corresponding transitions in the gas have been remeasured. At the onset of d-electron transitions, in both solid Kr and solid Xe, absorption-line series have been found, which have been identified as "forbidden" excitons in terms of Elliot's theory. At some distance from the onset, the broad maximum found earlier in gas absorption and ascribed to the delayed onset of $d \rightarrow f$ transitions can also be seen in the solids.

I. INTRODUCTION

OPTICAL measurements on the rare-gas solids have been restricted to the fundamental absorption region[1–5] up to 14 eV and to the vicinity of the K edge in Kr and Xe.[6] Electron energy-loss measurements have been performed up to 30 eV.[7–10] Apart from these energy ranges, no optical experiments have been reported. For the gaseous state, however, a large amount of experimental and theoretical material is now available for a wide spectral region. Comparison of optical data of rare-gas solids with those in the gaseous state promises new information on the influence of the solid state.

For transitions from the $4d$ shell in Xe gas, Ederer[11] has observed a delayed onset of absorption with a maximum at about 30 eV above threshold. This absorption behavior has theoretically been explained[12–14] as owing to a suppression of the $d \rightarrow f$ transitions near the threshold, which is caused by a centrifugal-repulsion potential superimposed on the attractive Coulomb potential. At a certain distance from the threshold, one can expect the atomic behavior to be a good approximation for the solid state. This has been used for interpretation of the spectra of several metals[14–17] and alkali halides,[18] but to our knowledge no direct experimental

* Work supported in part by the Deutsche Forschungsgemeinschaft.

† Present address: Department of Physics and Astronomy, University of Maryland, College Park, Md. 20742.

[1] G. Baldini, Phys. Rev. **128**, 1562 (1962).
[2] O. Schnepp and K. Dressler, J. Chem. Phys. **33**, 49 (1960).
[3] I. T. Steinberger and O. Schnepp, Solid State Commun. **5**, 417 (1967).
[4] D. Beaglehole, Phys. Rev. Letters **15**, 551 (1965).
[5] J. F. O'Brien and K. J. Teegarden, Phys. Rev. Letters **17**, 919 (1966).
[6] J. A. Soules and C. H. Shaw, Phys. Rev. **113**, 470 (1959).
[7] E. M. Hörl and J. A. Suddeth, J. Appl. Phys. **32**, 2521 (1961).
[8] H. Boersch, O. Bostanjoglo, and L. Schmidt, Tagung für Elektronenmikroskopie, Aachen, 1965 (unpublished).
[9] P. Keil, Z. Naturforsch **21a**, 503 (1966).
[10] P. Keil, Z. Physik **214**, 251 (1968).
[11] D. L. Ederer, Phys. Rev. Letters **13**, 760 (1964).
[12] J. W. Cooper, Phys. Rev. Letters **13**, 762 (1964).
[13] S. T. Manson and J. W. Cooper, Phys. Rev. **165**, 126 (1968).
[14] U. Fàno and J. W. Cooper, Rev. Mod. Phys. **40**, 441 (1968).
[15] R. Haensel, C. Kunz, T. Sasaki, and B. Sonntag, Appl. Opt. **7**, 301 (1968).
[16] B. Sonntag, R. Haensel, and C. Kunz, Solid State Commun. **7**, 597 (1969).
[17] P. Jaeglé and G. Missoni, Compt. Rend. **262**, 71 (1966).
[18] H. Fujita, C. Gähwiller, and F. C. Brown, Phys. Rev. Letters **22**, 1369 (1969).

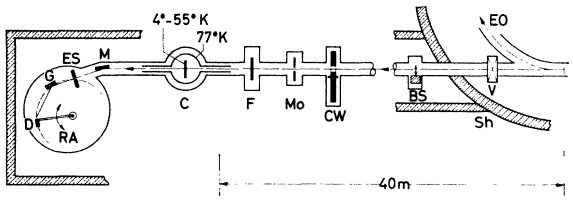

FIG. 1. Experimental arrangement: *EO* = electron orbit, *V* = valve, *Sh* = shielding, *BS* = beam shutter, *CW* = chopper wheel, *Mo* = monitor (Cu-Be sheet), *F* = filter, *C* = cryostat, *M* = mirror, *ES* = entrance slit of the Rowland monochromator, *RA* = rotating arm, *G* = grating, and *D* = detector (photomultiplier behind the exit slit).

comparison of one material in both states of aggregation has been performed to this day. Therefore, it seemed especially interesting to compare the continuum absorption of Xe in both the solid and the gaseous state.

Madden and Codling[19] have given a survey of the absorption structures in the rare gases near thresholds for transitions of different types. The corresponding transitions in the rare-gas solids should be explicable with the help of energy-band calculations and exciton theory. Fowler[20] has performed band calculations for solid Kr, and Reilly[21] for solid Xe. Band theory, however, only considers one-electron transitions and does not include excitons. Excitons may be described in the two limiting cases of small and large excitons with the help of the Frenkel model and the Wannier model.[22] An intermediate case can be expected[23] for the rare-gas solids, and Baldini[1] has, in fact, shown experimentally that excitons in the fundamental absorption region are not only close to the corresponding gas lines (Frenkel picture), but also form line series (Wannier picture).

In the following pages, a detailed description of the absorption behavior of solid Kr due to $3d$-electron transitions and of solid Xe due to $4d$- and $4p$-electron transitions will be given. As a comparison, the corresponding transitions have also been investigated in the gaseous state. The Xe $4d$ transitions near the threshold have already been published in a short letter,[24] but our results of Kr $3d$ transitions have led to a better understanding of these structures. Details of the experimental arrangement and of the procedure for obtaining the results will be given in Sec. II. In Sec. III the results will be presented and discussed with a view to experiments performed in the fundamental absorption region and to theoretical predictions.

[19] R. P. Madden and K. Codling, in *Autoionization: Astrophysical, Theoretical, and Laboratory Experimental Aspects*, edited by A. Temkin (Mono Book Corp., Baltimore, Md., 1966), p. 129.
[20] W. B. Fowler, Phys. Rev. **132**, 1591 (1963).
[21] M. H. Reilly, J. Phys. Chem. Solids **28**, 2067 (1967).
[22] R. S. Knox, in *The Theory of Excitons* (Academic Press Inc., New York, 1963).
[23] Y. Toyozawa, M. Inoue, T. Inui, M. Okazaki, and E. Hanamura, J. Phys. Soc. Japan **22**, 1337 (1967).
[24] R. Haensel, G. Keitel, P. Schreiber, and C. Kunz, Phys. Rev. Letters **22**, 398 (1969).

II. EXPERIMENTAL PROCEDURE

A. Light Source and Spectrometer

The measurements have been performed using the 7.5-GeV electron synchrotron DESY as a light source. The spectrum of synchrotron radiation extends continuously from the visible to the x-ray region. In the photon energy region 10–500 eV, the intensity is much higher than that of conventional (especially continuum) sources. Another advantage, especially for the experiments with samples cooled down to liquid-He temperature, is the good vacuum in the synchrotron. More details of the DESY synchrotron radiation may be found elsewhere.[25,26]

The light, concentrated in a narrow cone around the instantaneous flight direction of the electrons, comes through a beam pipe mounted tangentially to the electron orbit in a deflecting magnet. The spectrometer, cryostat, filters, etc., are mounted at a distance of 40 m from the tangential point at the accelerator. The experimental arrangement is shown in Fig. 1. The spectrometer used for our measurements is a 1-m Rowland mounting. The grazing angle of incidence was $\alpha = 219.6$ mrad for the Kr $3d$- and Xe $4p$-transitions measurements in the energy range 90–160 eV, and $\alpha = 304.1$ mrad for the Xe $4d$-transition measurements in the energy range 60–100 eV. The grating used has a line density of 2400 lines/mm and a blaze angle of 4° 16′. The resolution of the instrument, as derived from the width of the direct image, was approximately 0.1 Å. The energy calibration was based on gas-absorption lines (see Sec. III).

The radiation detector mounted behind the exit slit is an open photomultiplier (Bendix M 306) operated in the dc mode. To compensate for fluctuations of the

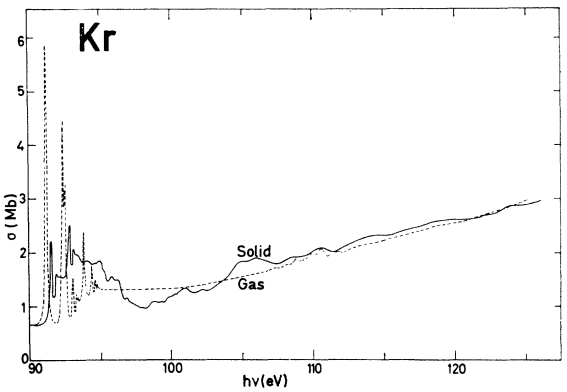

FIG. 2. Cross section versus photon energy for solid (solid curve) and gaseous (dashed curve) Kr in the energy range 90–128 eV. The cross section for gaseous Kr is given absolutely in Mb (10^{-18} cm^2) with an error of 10%. The curve for solid Kr is adjusted in such a way, that the integrated oscillator strengths become equal for both solid and gaseous Kr.

[25] R. Haensel and C. Kunz, Z. Angew. Physik **37**, 276 (1966).
[26] R. P. Godwin, in *Springer Tracts in Modern Physics*, edited by G. Höhler (Springer-Verlag, Berlin, 1969), Vol. 51, p. 1.

accelerator current, the photocurrent from a Cu-Be sheet, illuminated by synchrotron light, is taken as a monitor signal for the incoming intensity. Both intensity signals are amplified by lock-in amplifiers (Princeton Applied Research Model HR 8). DESY is operated by a 50-cps repetition rate. Every second pulse of the radiation is suppressed by a chopper wheel mounted in the beam pipe. Thereby, the light becomes modulated with 25 cps, and noise with 50 cps can be rejected by the tuned amplifiers. The ratio of both signals is formed in the y channel of a xy recorder, whose x axis is coupled to the wavelength-drive of the spectrometer.

In front of the entrance slit of the spectrometer, a concave mirror is mounted, which deflects the beam coming from the accelerator by about 10° and images the source onto the entrance slit. This increases the intensity coming into the spectrometer and reduces background from the high-energy part of the synchrotron radiation.

A further reduction of background, caused by light reflected from the grating into higher orders, is achieved by an appropriate angle of incidence to the grating (as mentioned above) and by using Al filters for the Xe $4d$-absorption measurements in solid Xe up to 73 eV (the $L_{II,III}$ absorption edge of Al).

B. Absorbing Samples and Data Reduction

For the absorption measurements of the rare-gas solids, a He cryostat was mounted between the source and the concave mirror. The gas was evaporated onto a 450-Å-thick carbon foil cooled down to a temperature just below the sublimation point (40°K for Kr and 55°K for Xe). To avoid contamination, the He-cooled region was surrounded by a N_2-cooled shield with 40-cm-long tubular extensions into both sides of the beam pipe. The pressure in the vacuum system outside the cryostat was kept below 10^{-6} Torr. In this way, no evidence of contamination of the carbon foils was found during the measurements (lasting 8 h on an average). The thicknesses of the rare-gas-solid films were not measured directly, but estimated by comparison with gas absorption (see Sec. III). Typical values ranged between 1000 and 10 000 Å. Such films were evaporated in about 1 min.

For the gas-absorption measurements, the cryostat was replaced by a 7.8-cm-long absorption cell with carbon windows on each side.[27] The pressures, which were measured by a precision membrane vacuum meter (Datametrics Model 1014), ranged from 2–5 Torr for Kr and from 0.1–1 Torr for Xe. The accuracy of the instrument is ±0.1%, the pressure was kept constant to ±2%.

The high-purity gas (99.999%) used in our experiments was of commercial origin (L'Air Liquide). All connections between the absorption cell and the gas reservoir were carefully evacuated to high vacuum before the gas was let into the absorption cell.

[27] H. Wöhl, Diplomarbeit, Universität Hamburg, 1968 (unpublished).

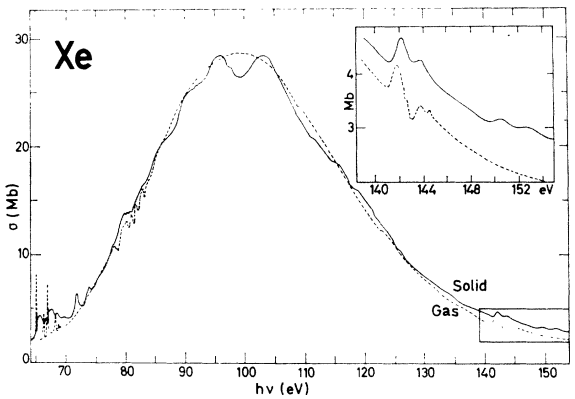

FIG. 3. Cross section versus photon energy for solid (solid curve) and gaseous (dashed curve) Xe in the energy range 64–155 eV. The cross section for gaseous Xe is given absolutely in Mb (10^{-18} cm^2) with an error of 10%. The curve for solid Xe is adjusted in such a way, that the integrated oscillator strengths become equal for both solid and gaseous Xe. The inset shows the cross sections in the region of $4p$-electron excitation in an extended scale.

The spectra recorded by the xy recorder were taken with and without absorbers, subsequently digitalized and handled by a computer. Wavelength calibration marks were directly read from a five-decimal digital voltmeter.

The measurement in the regions of different absorption coefficients have been performed with samples of different thicknesses and with different pressures in the absorption cell in order to check the accuracy of the data as well as to detect and to eliminate higher-order stray light. The relative accuracy in the spectral region below 130 eV is about 10%; in the region above 130 eV, the error is increasing continuously up to 25% since the intensity decreases. Differences in the absorption coefficient in the order of 1% were clearly detectable, if the photon energies were not more than some eV apart.

III. EXPERIMENTAL RESULTS AND DISCUSSION

The absorption curves of Kr from the onset of $3d$ transitions (90 eV) up to 128 eV are shown in Fig. 2 and the curves for $4d$ and $4p$ transitions (64–155 eV) in Xe are shown in Fig. 3. The over-all shape of the spectra—if one disregards the fine structure—is very similar for both gas and solid. This is especially evident for Xe, where a broad hump at 100 eV dominates the spectrum. In Kr our energy range was too small to cover the corresponding phenomenon. The onset is almost at the same energy for the gas and the solid. At higher photon energies, we find detailed fine structures of different shapes in both states. On the following pages, the absorption curves will be discussed in detail.

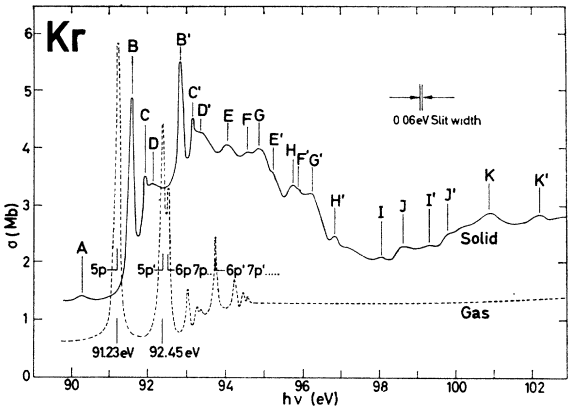

FIG. 4. Cross section versus photon energy for solid (solid curve) and gaseous (dashed curve) Kr near the onset of $3d$-electron excitation. The cross section for the solid has been multiplied by a factor of 2. In the gas, the members of the two spin-orbit splitted line series $3d^{10}4s^24p^6\,{}^1S_0 \rightarrow 3d^94s^24p^6({}^2D_{5/2})np\,{}^1P_1$ and $3d^{10}4s^24p^6\,{}^1S_0 \rightarrow 3d^94s^24p^6({}^2D_{3/2})np'\,{}^1P_1$ are denoted by np and np', respectively. In the solid, the most important structures are labeled with capital letters, unprimed and primed letters showing up spin-orbit pairs.

A. Continuum Absorption

As mentioned in Sec. I, the broad maximum in the absorption of gaseous Xe has for the first time been observed by Ederer[11] and has been explained by Cooper[12] as being caused by the delayed onset of the $d \rightarrow f$ transitions. Our results are in excellent agreement with those of Ederer[11] and of Lukirskii *et al.*,[28] whereas they differ somewhat from the calculated cross sections of Cooper[12] and McGuire.[29] The same is true for Kr, where the experimental values are in agreement with those of Lukirskii *et al.*[28] at 124 eV (=100 Å), but less in agreement with the theoretical values of McGuire.[29] The absolute error in the σ values of the gases in Figs. 2 and 3 is about $\pm 10\%$. At the higher-energy side, above 135 eV in Xe, the absolute accuracy is only $\pm 25\%$, since the intensity in the present adjustments of the spectrometer was too low for these photon energies (see Sec. II B).

Since for the solid Xe- and Kr-absorption measurements film thickness was not determined, the curves in Figs. 2 and 3 have been normalized in such a way that the total absorption integrated over the whole energy range is the same for the solids and the gases. In doing this, we find that the curves are in excellent agreement in both states of Kr and Xe before the onset of the d transitions (where residual absorption due to transitions from the outer shells to high-lying states in the continuum occurs). Moreover, there is good agreement in the whole continuum absorption range, which is especially striking in Xe where both humps occur at the same photon energy. We have estimated the accuracy with which we are able to prove this over-all agreement to be 10% below 130 eV. Only near the onset of $4p$ transitions in Xe is the agreement somewhat less, but this may be explained by the reduced absolute accuracy.

B. Excitonic Structure near Onset of d Transitions

Krypton

Figure 4 shows a detailed view of Fig. 2 near the onset of transitions from the $3d$ shell of Kr. In the gas curve, we see two series of lines caused by the spin-orbit splitting of the $3d$ shell (1.22 eV; see Ref. 30), namely,

$$3d^{10}4s^24p^6\,{}^1S_0 \rightarrow 3d^94s^24p^6({}^2D_{5/2})np\,{}^1P_1 \quad (n \geq 5;\ \text{first member } 91.23 \text{ eV})$$

and

$$3d^{10}4s^24p^6\,{}^1S_0 \rightarrow 3d^94s^24p^6({}^2D_{3/2})np'\,{}^1P_1 \quad (n \geq 5;\ \text{first member } 92.45 \text{ eV}).$$

Codling and Madden[30] have given the energy positions of these gas-absorption lines on which our energy calibration is based.

In solid Kr, a weak peak A can be seen at 90.28 eV followed by many absorption structures. These structures occur in pairs with energy distances of about 1.2 eV, the $3d$ shell spin-orbit splitting energy. The maxima are labeled with unprimed and primed letters. Table I gives the energy positions of the most prominent ab-

TABLE I. Energy positions of the most prominent structures in solid Xe and solid Kr.

Structure	Energy (eV) Solid Xe	Solid Kr
A	64.36±0.08	90.28±0.08
B	65.28±0.04	91.61±0.04
B'	67.24±0.04	92.90±0.04
C	65.48±0.05	91.99±0.04
C'	67.53±0.1	93.22±0.04
D	65.87±0.08	92.13±0.05
D'	67.87±0.05	
E	66.60±0.08	94.19±0.05
E'		95.34±0.08
F	66.79±0.05	94.62±0.08
F'	68.68±0.05	
G	69.98±0.05	94.96±0.05
G'		96.28±0.1
H	72.17±0.07	95.82±0.06
H'	74.19±0.07	96.97±0.06
I		98.18±0.06
I'		99.47±0.06
J		98.75±0.06
J'		
K		101.05±0.06
K'		102.33±0.06

[28] A. P. Lukirskii, I. A. Brytov, and T. M. Zimkina, Opt. Spektroscopiya **17**, 438 (1964) [English transl.: Opt. Spectry. (USSR) **17**, 234 (1964)].

[29] E. J. McGuire, Phys. Rev. **175**, 20 (1968).

[30] K. Codling and R. P. Madden, Phys. Rev. Letters **12**, 106 (1964).

sorption structures. Peaks B, C and B', C' are of special interest. They are especially sharp, the width being comparable to that of the gas-absorption lines. B and B' are very close to the first members of the gas-absorption lines, but their oscillator strengths are much smaller. In analogy to the situation in the fundamental absorption region,[1] we believe that B, C and B', C' are members of a Wannier exciton series.

Besides those excitons which are responsible for the structure in the fundamental absorption region[1] and which are formed at band singularities between which optical interband transitions are allowed, there can exist, according to Elliot,[31] a second class of excitons ("forbidden" excitons) at critical points, where optical interband transitions are forbidden. These excitons also show hydrogenlike Rydberg series of absorption lines, but $n=1$ is missing. According to Fowler's band calculation,[20] the lowest point of the conduction band in solid Kr is the s-symmetric Γ_1 point. Since the lowest point with odd symmetry accessible for first class excitons can only be found several eV above the bottom of the conduction band, we believe that B,B' and C,C' are the $n=2$ and $n=3$ members of a second-class exciton series coupled to Γ_1.

According to a Rydberg formula, the Wannier series form hydrogenlike series such as

$$E=E_0-E_b/n^2 \quad \text{with} \quad E_b=e^4\mu/2\hbar^2\epsilon^2, \qquad (1)$$

where E is the exciton energy, E_0 is the series' limit, E_b is the exciton binding energy, μ is the reduced exciton mass and ϵ the dielectric constant. The binding energy E_b for a second-class series is found to be 2.7 eV for the first series (B,C) and 2.3 eV for the second (B',C'); consequently, E_0 is 92.3 and 93.5 eV. The binding energies for the corresponding first-class valence-band excitons are, according to Baldini,[1] 1.7 and 1.5 eV. The higher values for the core-exciton binding energies are intelligible because of the higher effective mass μ. Were the peaks B and C to be $n=1$ and $n=2$ members of a first-class exciton series, then the calculation of E_b would give only 0.5 and 0.4 eV, which would be unreasonably low. Thus, peak A would now be understandable as being the theoretically forbidden $n=1$ member, which is not completely suppressed, due perhaps to crystal imperfections in the solid Kr film. Its energy position at 90.28 eV is not exactly what it should be if calculated according to Eq. (1) (namely 89.56 eV), but such a deviation is usually the case for the $n=1$ exciton.[1]

These considerations imply the applicability of the Wannier exciton theory.[22,31] However, core excitons may have binding energies comparable to the band-gap energy, in which case the Wannier theory should break down. In such a case the assignment of exciton peaks to distinct points of the Brillouin zone would be meaningless.

[31] R. J. Elliot, Phys. Rev. **108**, 1384 (1957).

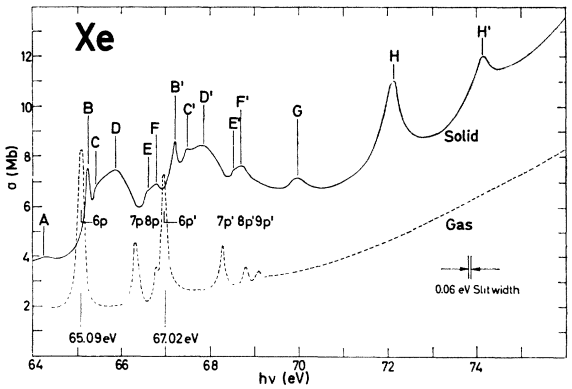

FIG. 5. Cross section versus photon energy for solid (solid curve) and gaseous (dashed curve) Xe near the onset of $4d$-electron excitation. The cross section for the solid has been multiplied by a factor of 2. In the gas, the members of the two spin-orbit splitted line series $4d^{10}5s^25p^6\,{}^1S_0 \rightarrow 4d^95s^25p^6({}^2D_{5/2})np\,{}^1P_1$ and $4d^{10}5s^25p^6\,{}^1S_0 \rightarrow 4d^95s^25p^6({}^2D_{3/2})np'\,{}^1P_1$ are denoted by np and np', respectively. In the solid, the most important structures are labeled with capital letters, unprimed and primed letters showing up spin-orbit pairs.

Xenon

These conclusions lead to the assumption that a similar situation occurs near the threshold of the $4d$ transitions in Xe. Figure 5 shows a detailed view of the low-energy region in Fig. 3 (preliminary results have been published before[24]). In the gas-curve two line series,

$$4d^{10}5s^25p^6\,{}^1S_0 \rightarrow 4d^95s^25p^6({}^2D_{5/2})np\,{}^1P_1$$
($n\geq 6$; first member 65.09 eV)

and

$$4d^{10}5s^25p^6\,{}^1S_0 \rightarrow 4d^95s^25p^6({}^2D_{3/2})np'\,{}^1P_1$$
($n\geq 6$; first member 67.02 eV)

can be seen converging at 67.55 and 69.52 eV, thus giving a spin-orbit splitting energy for the $4d$ shell of 1.97 eV.[30]

In solid Xe, in accordance with Kr, B, B' and C, C' are also assumed to be the first members of a second-class series. The structure C is not as clear as in solid Kr and, therefore, $E_b=1.4$ eV and $E_b'=2.1$ eV as well as $E_0=65.6$ eV and $E_0'=67.8$ eV are not so well established. Again, peak A would be the not completely suppressed $n=1$ exciton. According to Reilly's band calculations,[21] which are very similar to those of solid Kr, the bottom of the conduction band has even parity and the first odd-parity states are at 5 eV higher energies.

Other Discrete Structures

Beyond the first excitons in solid Kr and Xe, other discrete structures are to be seen in Figs. 2–5. They may be metastable excitons or van Hove singularities in interband transitions. An assignment to specific singularities in the conduction band, however, is impossible at the present time.

In the gas-absorption curves of Figs. 2 and 3, some structures can be found for Kr near 110 eV and for Xe near 80 eV, which have previously been observed by Codling and Madden,[32] who ascribed these to double excitation of electrons in the d and outer p shell. In the same region, the absorption curves of solid Kr and Xe also show specific structures which are especially evident in solid Xe. As in the case of the gas, their oscillator strengths are much weaker than that of the single d-electron transitions.

In this connection it should be noted that Hermanson[33] made an estimation of double quantum-excitation probability on alkali halides with the result that it should be weaker by two orders of magnitude than that of single quantum excitations. This is in contrast to Miyakawa,[34] who stated that both types of excitations should occur with similar probability. Our present results together with recent photoemission data[35] are in favor of Hermanson's theory. The onset of transitions from the $4p$ shell in Xe around 140 eV can be seen in the inset of Fig. 3. The gas structure has already been investigated by Codling and Madden.[32] In agreement with our own results for gaseous Xe, the authors only find evidence of transitions from the $4p\frac{3}{2}$ shell. They ascribe the absence of structures from $4p\frac{1}{2}$ shell transitions to the fact that these contributions are deep in the $4p\frac{3}{2}$ continuum, since the spin-orbit splitting energy of $4p$ is expected to be relatively large (about 8 eV). This should substantially decrease the lifetime of discrete states formed by transitions from the $4p\frac{1}{2}$ shell. It is, therefore, very surprising that in solid Xe, at about 150 eV, two peaks can be seen similar to those at 142 eV. They are obviously due to transitions from the $4p\frac{1}{2}$ shell.

[32] K. Codling and R. P. Madden, Appl. Opt. **4**, 1431 (1965).
[33] J. C. Hermanson, Phys. Rev. **177**, 1234 (1969).
[34] T. Miyakawa, J. Phys. Soc. Japan **17**, 1898 (1962).
[35] R. Haensel, G. Keitel, C. Kunz, G. Peters, P. Schreiber, and B. Sonntag Phys. Rev. Letters **23**, 530 (1969).

ACKNOWLEDGMENTS

The authors are grateful to the directors of the Deutsches Elektronen-Synchrotron and the Physikalisches Staatsinstitut, particularly to Professor P. Stähelin, for continuous interest in this work and for valuable support of the synchrotron radiation group. Thanks are also due to H. Dietrich, M. Lehnert, D. Michael, G. Singmann, and E. W. Weiner for technical assistance during the course of experiments. Stimulating discussions on the subject with G. Baldini, M. Cardona, J. J. Hopfield, D. W. Lynch, Y. Onodera, and B. Sonntag and comments by R. P. Madden, M. H. Reilly, and V. Röbeer are gratefully acknowledged.

PHYSICAL REVIEW VOLUME 188, NUMBER 3 15 DECEMBER 1969

Exciton and Interband Spectra of Crystalline CaO†

R. C. WHITED AND W. C. WALKER
Physics Department, University of California, Santa Barbara, California 93106
(Received 24 July 1969)

Absolute, near-normal-incidence reflectance spectra were obtained for CaO at 300°K from 6 to 35 eV and at 80 and 25°K from 6 to 12 eV. The important optical parameters were obtained by Kramers-Kronig inversion of the reflectance spectra. The ϵ_2 spectrum of CaO at 25°K showed two strong-exciton peaks at 6.79 and 11.42 eV, a set of weak-exciton doublets, and strong-interband peaks at 10.0, 12.1, and 16.9 eV. Interband structure observed in the ϵ_2 spectrum of CaO was associated with specific transitions by analogy with the band structure of MgO. The main features of the resulting band structure were: (1) The first conduction band of CaO is about 1 eV lower than in MgO; (2) the X_3 point of the second conduction band is lowered by about 7 eV from that in MgO.

I. INTRODUCTION

ALTHOUGH much of the early work on oxide-coated cathodes involved the use of calcium oxide, few data relating to the electronic structure of the material have appeared in the modern literature. Janin and Cotton[1] observed a threshold for photoconductivity in a thin disk of powered calcium oxide at about 6.2 eV. Relatively large photocurrents were observed when the sample was irradiated by 6.7-eV light. In 1963, Neeley and Kemp[2] measured the optical absorption of CaO single crystals in the range 14.5 μ to 2000 Å. They found uv absorption bands beginning at approximately 2500 Å and infrared bands beginning at 10 μ. Glascock and Hensley[3] measured the room-temperature optical absorption of thin films of CaO backed by LiF or fused-quartz plates in the energy

† Work supported by the National Aeronautics and Space Administration.
[1] J. Janin and L. Cotton, Compt. Rend. **246**, 1936 (1958).
[2] V. I. Neeley and J. C. Kemp, J. Phys. Chem. Solids **24**, 1301 (1963).
[3] H. H. Glascock and E. B. Hensley, Phys. Rev. **131**, 649 (1963).